Targeting the unstable atherosclerotic plaque : diagnostic and therapeutic implications

Segers, F.M.E.

Chapter 3

Targeting Inflammatory Plaques by a Novel Phage Display Derived Peptide Ligand for the CD40 Receptor

Filip M.E. Segers*[1], Haixiang Yu*[1], Karen Sliedregt-Bol[2], Ilze Bot[1], Andrea M. Woltman[3], Peter Boross[4], Sjef Verbeek[4], Herman S. Overkleeft[2], Gijs A. van der Marel[2], Cees van Kooten[3], Theo J.C. van Berkel[1], and Erik A.L. Biessen[1,5]

(*Both authors contributed equally)

[1] Division of Biopharmaceutics, Leiden/Amsterdam Center for Drug Research, Leiden University, Leiden, The Netherlands
[2] Leiden Institute of Chemistry and Netherlands Proteomics Center, Gorlaeus Laboratories, Leiden University, Leiden, The Netherlands
[3] Department of Nephrology, Leiden University Medical Center, Leiden, The Netherlands
[4] Human and Clinical Genetics, Leiden University Medical Center, Leiden, The Netherlands
[5] Department of Pathology, Cardiovascular Research Institute Maastricht, Maastricht University, Maastricht, The Netherlands

(Submitted for publication)

Abstract

Background - The CD40/CD40L dyad is deemed to play a central role in several immunogenic and inflammatory processes, including atherosclerosis. As CD40 is overexpressed in atherosclerotic lesions and interruption of CD40 signalling was found to retard atherogenesis and stabilize vulnerable plaques, we sought to investigate the potential of CD40 as target for molecular imaging approaches in inflammatory disorders such as atherosclerosis.

Methods and Results - We designed a novel, selective peptide ligand for CD40 by phage display. Enriched phage pool selectively bound human CD40 and homed to inflammatory joints in a murine model of rheumatoid arthritis. Synthetic peptides corresponding with the phage insert, termed NP31, displayed nanomolar affinity for CD40. Affinity was further enhanced after docking onto a tetrameric streptavidin scaffold. A minimal essential 11-mer peptide motif was defined by truncation and alanine scan studies. Although NP31 was unable to interdict CD40L binding, it ablated VEGF transcriptional activation and partially inhibited IL-6 production by CD40L activated endothelial cells. Importantly NP31 did not only alter the biodistribution profile of a streptavidin scaffold but also markedly increased accumulation of the carrier in aortic lesions in a CD40 dependent manner.

Conclusions - The here described potent and selective peptide ligand for CD40 may have potential for targeted imaging and drug delivery approaches in CD40 dependent inflammatory disorders such as atherosclerosis.

Introduction

The CD40/CD154 (CD40 ligand, CD40L) dyad plays a central role in several immunogenic and inflammatory processes, including atherosclerosis[1-5]. Expression and function of CD40/CD154 are not restricted to B and activated T cells where it is involved in lymphocytic communication, but was seen to extend to a variety of other cell types relevant to atherosclerosis, such as monocytes, macrophages, dendritic cells, platelets, mast cells, fibroblasts, endothelial cells, and smooth muscle cells[6-8]. Ligation of CD40 triggers the expression of cytokines, adhesion molecules, growth factors, matrix metalloproteinases, tissue factors and apoptotic mediators[9-12]. Accordingly, CD40 signalling has been associated with the pathophysiology of immunodeficiency, collagen-induced arthritis, neurodegenerative disorders, graft-versus-host disease, cancer, and atherosclerosis[13-18]. Disruption of CD40/CD154 led to inhibition of immune responses and, in keeping, blockade of CD40/CD154 by monoclonal antibodies was seen to be beneficial in the treatment of autoimmune diseases[18], transplantation[19, 20] and atherosclerosis[17, 21, 22]. However, antibody therapy to interrupt CD40/CD154 signalling was accompanied with thromboembolic symptoms, which has raised major concerns for, and in fact precluded, further clinical studies on CD40 therapy in humans[23]. Therefore, alternative, more selective strategies to intervene in CD40 signalling are eagerly awaited.

The abundant expression of CD40 at sites of inflammation such as atherosclerotic lesions and its causal involvement in disease progression also renders CD40 a promising target for molecular imaging and targeted drug delivery approaches. In particular when aiming at the vulnerable plaque, CD40 directed molecular imaging may offer clear advantages as it will allow a more accurate detection of CD40-dependent inflammatory processes that are a typical feature of these plaques than mere detection of macrophage or lipid deposition. In this study, we used phage display, a powerful strategy for unbiased design of novel ligands, to identify selective peptide antagonists for human CD40 and showed the promise of newly identified peptides for CD40 targeted imaging of rheumatoid arthritis and atherosclerosis.

MATERIALS AND METHODS

Phage libraries

The cysteine-constrained peptide phage library pComb8 $CX_{15}C$, at which X is any amino acid, was generated at the Department of Biochemistry, University of Amsterdam, the Netherlands. The pIF15 phage library containing randomized linear 15-mer amino acids peptide sequence was kindly provided by Dr. Monaci, IRBM, Rome, Italy.

Antibody and plasmid

Goat anti-mouse IgG (Fc specific) antibody was from Sigma (St. Louis, MO, USA). Human CD40-murine IgG recombinant protein was from Ancell (Bayport, MN, USA). Human CD4-murine IgG was kindly provided by Dr. Appelmelk (Vrije Universiteit, Amsterdam, the Netherlands). Biotin, streptavidin, horseradish peroxidase conjugated streptavidin (StrepHRP) was from Amersham Bioscience (Buckinghamshire, England). Streptavidin-R-phycoerythrin (StrepPE) was from Sigma (St. Louis, MO, USA). Recombinant human soluble CD40L and murine soluble CD40L were from Santa Cruz (CA, USA). A VEGF-luciferase reporter construct (a kind gift of Dr. Yu-Tzu Tai, Harvard Medical School) containing genomic fragment of the human VEGF gene promoter (base pairs -2274 to +745; pVEGF-Luc) was used for reporter assays as described[24].

Cell culture

Mouse fibroblast L-CD40 cells stably transfected with human CD40 and negative control L-cells (ATCC: CCL 1.3, murine fibroblasts) were cultured as described[25]. Human Ea.Hy.926 and murine H5V endothelial cells were cultured in Dulbecco's modified Eagles's medium (DMEM) supplemented with 10% (v/v) heat-inactivated fetal bovine serum (FBS), 100U/mL penicillin, and 100µg/mL streptomycin.

Selection of CD40 binding phage

10 µg/mL of goat anti-mouse IgG in coating buffer (50mmol/L $NaHCO_3$, pH 9.6) was incubated overnight at 4°C in a high binding 96 well plate (Costar, Corning, UK) at 100 µL/well. Subsequently, wells were washed 3x with 200µL assay buffer (20mmol/L HEPES, 150mmol/L NaCl, 1mmol/L $CaCl_2$, pH7.4) and incubated for 1h at 37°C with 200µL blocking buffer (3% BSA in assay buffer). Wells were then incubated with 100µL 3µg/mL of human CD40-IgG in 100µL of binding buffer (0.1% BSA, 0.5% Tween 20 in assay buffer, 2h 37°C). After incubated for 2h at room temperature (RT) with the phage libraries at 10^9 colony forming units (CFU) in 100µL of binding buffer, wells were washed 10x with 200µL binding buffer and bound phage were eluted by incubation for 5 min at RT with 100µL of elution buffer (0.1mol/L glycine/HCl, pH2.2) and neutralized by addition of 50µL of neutralization buffer (1mol/L Tris/HCl, pH8.5). Phage were titrated, amplified and purified as described[26]. Amplified phage was used in further selection rounds. For DNA sequencing of enriched phage pools, plasmid DNA was isolated from

single colonies using the Wizard plus SV Miniprep DNA Purification System (Promega, Madison, USA). DNA sequencing of the plasmids was conducted at the DNA-sequencing facility of Leiden University Medical Center using standard M13 primers. Unless otherwise stated, the phage pool amplified from a single phage clone isolated after 5 rounds of selection was used for all further experiments.

Peptide synthesis

NP31 (CMSYEGSWRKWVMWGGCG), scrambled NP31 control peptide (NP31c, CEMGWMWGWRGSKYSVCG), biotinylated NP31 (CMSYEGSWRKWVMWGGCGGGK-biotin, truncated and alanine mutated NP31 peptides were synthesized by Fmoc solid-phase peptide synthesis on a Multisyntech Syro Multiple Peptide Synthesizer. Crude peptides were purified by a preparative C_{18} RP-HPLC (Alltech) on a BIOCAD VISION automated purification system. Purified peptides were characterized by LC-MS, MALDI-TOF MS and found to be at least 99% pure.

Competition experiment of CD40 selective phage binding

In analogy to the phage selection procedure, 10µg/mL of goat anti-mouse IgG in coating buffer was incubated overnight at 4°C in a high-binding 96-well plate, 100µL/well. Wells were washed 3x with assay buffer and incubated for 1h at 37°C with blocking buffer. After incubation for 2h at 37°C with 3µg/mL of human CD40-IgG (100µL/well), wells were washed 3x with binding buffer, after which the enriched phage pool at 10^9cfu in 100µL binding buffer was added and incubated for 2h at RT in the presence of NP31 or NP31c peptides. Wells were washed 10 fold with binding buffer and bound phage were eluted by incubation for 5 min at RT with 100µL elution buffer and neutralized with 50µL neutralization buffer. Residual phage binding was calculated from the output/input ratio.

Competition ELISA of selective peptide binding to CD40

Streptavidin-horseradish peroxidase (StrepHRP) was incubated for 2h at RT in phosphate-buffered saline (PBS) (pH7.0) with NP31-biotin at a 1:4 molar ratio, thus forming a tetrameric NP31-strepHRP complex. For competition studies, high binding microtiter wells were coated with human CD40-IgG as described under "Selection of CD40 binding phage". Wells were incubated for 1h at 4ºC with 250nmol/L NP31-strepHRP in assay buffer in the presence or absence of tittered amount of peptides. After washing 6x with 200µL assay buffer, the wells were incubated for 15min at RT with 100µL TMB/H_2O_2 (Pierce, Rockford, USA). The reaction was stopped by adding 50µL 2mol/L H_2SO_4 and absorbance read at 450nm. The inhibitory potency of the peptides was expressed as percentage of the specific NP31-strepHRP binding in the absence of peptide after correction for background binding.

NP31 peptide selectively binds to cells overexpressing CD40

L-cells stably transfected with human CD40 and CD40 null control L-cells were collected by centrifugation. 3×10^5 cells were suspended in 100 µL phosphate buffered saline containing 1% normal mouse serum and incubated in v-shape 96 well plate for 1h at 4ºC. NP31-strepPE and strepPE-biotin complex was freshly prepared by incubating strepPE for 2h at RT with NP31-biotin or biotin at a 1:4 molar ratio. After 2x washing with 100µL PBS, cells were incubated with 50µL (250nmol/L) StrepPE-biotin or strepPE-NP31 for 1h at 4°C. Cells were then washed 3x by 100µL PBS, resuspended in 150µL PBS, and then subjected to FACS analysis.

IL-6 cytokines production in endothelial cells

Cells cultured in 24 well plates were treated with and without sCD40L (10ng/mL) in the presence of NP31 peptide at indicated concentrations. After 24h, IL-6 that had been released into the culture medium was measured by ELISA (BD Biosciences Pharmingen, USA).

VEGF-luciferase reporter assay

Cells were seeded at 1×10^5 cells per well in 24 well plates for 24h. pVEGF-luc was cotransfected with pRL-CMV reference plasmid (encoding renilla luciferase) using transfection reagent ExGen 500 (MBI Fermentas) as previously described[27]. Cells were incubated at 37°C for at least 24h and then stimulated for 12h by shCD40L in the absence or presence of synthetic peptide. Cell lysates were prepared and simultaneously assayed for firefly and renilla luciferase activity using the Dual Luciferase Assay System (Promega) on a Turner Luminometer.

^{35}S-labeled CD40 selective binding phage effectively home to inflamed joints in a K/BxN arthritis mouse model

K/BxN mouse model (maintained on a C57Bl/6 background) was set up in the Department of Human and Clinical Genetics, Leiden University Medical Center, the Netherlands. In brief, repeated injection of 200µL sera from arthritic K/BxN mice into healthy C57Bl/6 recipients induces acute joint damage and cartilage erosion in the bone within a week[28]. The number of swollen paws per mouse was scored (maximum arthritis score: 4 per mouse). Mice with a score of 3 or higher were considered arthritic and used in further experiments. CD40 specific binding phage pool NP31 and non-specific control phage eluted from the second round of selection were radiolabeled as previously described[29] and injected at 10^9 CFU (~200,000 DPM) in 100µL Tris-buffered saline via the tail vein into anesthetized C57BL/6 mice or K/BxN mice suffering from joints inflammation (20 weeks old; male; n=3). After 2h, mice were subsequently perfused for 2min with DMEM and PBS at 10mL/min via a cannula inserted in the left ventricle. Organs were removed and weighed. Organ homogenates were obtained by overnight incubation of ~0.1g tissue with 500µL Solvable at 56ºC (Packard bioscience, Groningen, the Netherlands) and analyzed for associated ^{35}S radioactivity in a beta counter.

In vivo organ distribution of CD40 selective peptide ligand

ApoE$^{-/-}$ (41 ± 6.9 weeks old, chow diet) mice with advanced atherosclerotic lesions were via the tail vein injected with 1.7 pmol radiolabeled ^{125}I-Strep-NP31 (n=5) or [^{125}I]-Strep-biotin (n=5) in 100µl 0.9% sodium chloride (NaCl). After 1h circulation, mice were sacrificed and perfused with PBS. Organs were removed, weighed and radioactivity was analyzed using a Wizard 1470 automatic gamma counter (Perkin Elmer, USA). Aorta and kidney were removed and fixed in 4% formalin. Aortas were stained for lipids using Oil Red O (ORO) for 30 seconds and plaque size was characterized as a ratio of relative ORO stained lesion to total aortic area. Aortas were subsequently subjected to exposure in a phosphor screen at RT for one week. The intensity of the signal was quantified using ImageQuant software (Bio-Rad Laboratories, Hercules, CA), and the results were corrected for injected dose (cpm) and ORO positive stained area. Microsections (7 and 10µm) of kidney were prepared and were incubated for 1 week with a Kodak BioMax MR film (Sigma, St. Louis, MO) to detect ^{125}I signal.

NP31 uptake and colocalization with CD40 in atherosclerotic lesions

Biotinylated NP31 was docked on a PE labelled streptavidin (0.40µM, BD, USA) in a 5:1 ratio, and was intravenously injected in 1-year old ApoE$^{-/-}$ mice (n=2). After 1h circulation the mice were perfusion fixed with PBS and then 4% formalin through the left cardiac ventricle. Serial Cryosections (7 µm, n=4) of aortic valve area were prepared. Immunohistochemical staining was performed using a CD40 rabbit polyclonal antibody (1:100, Abcam, Cambridge, UK), an Alexa488 labelled goat anti-rabbit secondary Ab (1:100, Molecular Probes Inc., Eugene, OR) and a nuclear DAPI staining (Serva Feinbiochemica, Heidelberg, Germany). Slides were mounted with Fluorescence Mounting Medium (DAKO Netherlands B.V., Heverlee, Belgium) and analyzed using a Bio-Rad Radiance 2100 MP confocal laser scanning system equipped with a Nikon Eclipse TE2000-U inverted fluorescence microscope.

Statistical Analysis and animal handling ethics

Values are expressed as mean ± S.E.M. A two-tailed unpaired Student's t-test was used to compare individual groups. A level of $P<0.05$ was considered significant. Animal experiments were performed at the Gorlaeus laboratories of the Leiden/Amsterdam Center for Drug Research in accordance with the National Laws. All experimental protocols were approved by the Ethics Committee for Animal Experiments of Leiden University.

RESULTS

Screening of phage displayed peptide libraries against human CD40

Peptide phage libraries pIF15 and pComb8, encoding random linear and cysteine-constrained 15-mer peptide sequences respectively, were screened for novel human CD40 binding peptide sequences. To favor selection of peptides binding to the actual binding pocket of CD40, biopanning was performed on wells coated with anti-mouse IgG docked human CD40/murine IgG fusion protein, comprising the 173 amino acid extracellular domain of CD40. The selection pressure was increased from round three onwards by applying more stringent washes combined with 10-fold reduced coating densities of CD40-IgG. This strategy led to approximately 200-fold enrichment of CD40 binding phage for the pComb8 constrained library in the 5th round (figure 3.1A).

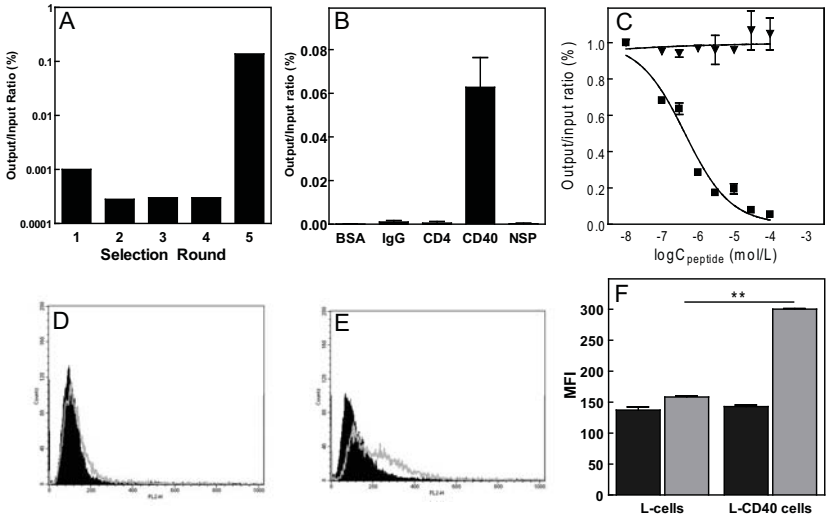

Figure 3.1 Screening and selectivity of CD40 binding phage. (A) Selection of the pComb8 phage displayed peptide library on immobilized human CD40 recombinant protein led to a sharp enrichment of human CD40 binding phage in the 5th round of selection (~200 fold increase) **(B)** In comparison to a nonspecific phage pool, the enriched phage pool specifically bound to human CD40-IgG but not to immobilizing agent anti-mouse Ig, blocking agent BSA or human CD4-IgG fusion protein. Phage binding is expressed as ratio of output to input and represent means ±SD of three individual experiments. **(C)** Binding of the enriched phage pool to human CD40-IgG was determined in the presence of synthetic peptides encoded by CD40 specific phage clone NP31 (■); a scrambled NP31 sequence was used as control peptide (▼). IC_{50} values, as calculated from the competition curves were 440 nmol/L. Phage binding is expressed as ratio of output to input and represent means ±SD of three individual experiments. Streptavidin-PE conjugated NP31 complexes selectively and avidly bound to cells overexpressing human CD40. CD40$^-$ L-cells **(D)** or L cells stably transfected with human CD40 **(E)** were incubated for 1 h at 4ºC with freshly prepared NP31-strepPE or strepPE-biotin (250 nmol/L). After washing with PBS, cells were resuspended and subjected to FACS analysis. Black histogram: strepPE-biotin, Open histogram: NP31-strepPE. **(F)** Mean fluorescence intensity of PE$^+$ cells was calculated as a measure of CD40 specific binding of strepPE-biotin (black bars) and NP31-strepPE (open bars). Values represent means±SD of three individual experiments.

DNA sequence analysis of the CD40 binding phage clones isolated after 5 rounds of selection from the pComb8 library revealed a single 15-mer cyclic peptide sequence (CMSYEGSWRK*WVMWG*GC), termed NP31, in 5 out of 5 phage clones for the cystine constrained pComb8 library. Sequencing of phage clones isolated

after 4 rounds of selection gave multiple peptide sequences with a shared motif (see table 1), the most prominent being NP31, NP58 and NP26 (sequence ratio 3:1:1). Interestingly, parallel phage display of a non-constrained pIF15 linear 15-mer peptide library resulted in the identification of a consensus peptide sequence NP2 containing a WRK consensus motif. Discontinuous Blast search for homology showed that the ABC transporter permease protein contains a WVMWG motif.

Selectivity of CD40 specific binding phage NP31

The specificity of the enriched phage pool was tested in an ELISA based binding assay onto coated recombinant human CD40-IgG. Of the selected phage clones NP2, NP26, and NP58 were found to interact with human CD40 in a rather non-specific manner, either binding immobilising antibody or the polystyrene plate. In contrast, the enriched phage pool NP31 showed selective binding to anti-mouse IgG immobilized human CD40 (figure 3.1B). NP31 phage did not bind to the blocking agent BSA, anti-mouse IgG alone or immobilized human CD4. As expected, the non-selected parental phage library showed little binding, confirming the specificity of NP31 for recombinant human CD40.

Potency and selectivity of phage encoded synthetic NP31 peptides for CD40

We synthesized a cyclic peptide (NP31), corresponding with the peptide insert of the CD40 specific phage clone. The capacity of NP31 to interfere with NP31 phage binding to human CD40 was tested in a competition assay (figure 3.1C). NP31 dose-dependently and potently inhibited binding of the enriched phage pool to human CD40 at a calculated IC_{50} of 440nmol/L, whereas the scrambled control NP31c was completely ineffective up to 100µmol/L. We next verified whether NP31 was also able to bind full length CD40 receptor expressed on cells. Concordant with the observation that CD40 interacts with CD40L as trimer or preformed trimer[30], it was reported to display a similar preference for oligomeric ligands[31]. Hence we have docked NP31, biotinylated at its C-terminal end, to a streptavidin-PE scaffold, generating a tetrameric NP31-strepPE complex. We have investigated the ability of strepPE-biotin or NP31-strepPE to bind murine fibroblast L-cells (figure 3.1D) or L-cells overexpressing human CD40 (figure 3.1E) by flow cytometry. Quantitative results are given in figure 3.1F. After conjugation to the streptavidin-PE scaffold, NP31 showed significantly higher binding to $CD40^+$ L-CD40 cells than to $CD40^-$ L-cells ($P<0.001$) at concentrations as low as 250nmol/L. A strepPE-biotin control did not give any differential binding to $CD40^+$ and $CD40^-$ cells. In fact the binding of strepPE-biotin to L-CD40 cells was very similar to that of NP31-StrepPE to $CD40^-$ L-cells and significantly lower than that of NP31-strepPE to $CD40^+$ L-cells.

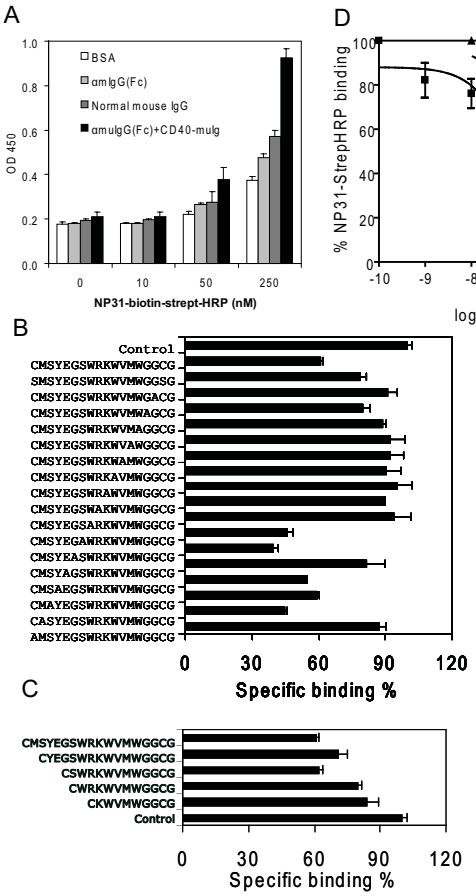

Figure 3.2 Identification of the minimal essential binding motif of NP31 peptide. (A) NP31 binding studies were performed in an ELISA. NP31-strepHRP (250 nmol/L) selectively bound to immobilized (3 µg/mL) human CD40-IgG, but not to coated anti-mouse IgG, BSA or normal mouse IgG (3 µg/mL). **(B)** Competition studies of NP31-strepHRP binding to CD40 by synthetic NP31 (▲) revealed an IC50 value of 215 nmol/L. NP31, when presented as a tetramer on streptavidin, displayed a 2.5 fold higher affinity for CD40 (■). The inhibitory capacity of alanine mismatched **(C) or** truncated **(D)** analogues of NP31 for CD40 was measured in the NP31-strepHRP ELISA. Binding was expressed as percentage of specific NP31-strepHRP binding after correction for background binding. Values represent means ±SD of three individual experiments.

Identification of the minimal essential motif of CD40 binding peptide

Based on the partial sequence homology of the linear and cyclic peptide inserts of the various isolated phage clones, we assumed that recognition of human CD40 may only implicate part of the NP31 peptide sequence. To characterize the peptide-CD40 interaction more closely, we set up an ELISA based on binding of a preformed complex of biotinylated NP31 and streptavidin-HRP (NP31-strepHRP) to anti-mouse IgG docked CD40. NP31-strepHRP bound avidly to immobilized human CD40 at 250nmol/L (figure 3.2A). In addition, NP31-strepHRP showed only basal interaction with anti-mouse IgG, with the blocking agent BSA or with normal mouse IgG, which served as negative control, indicating that NP31 binding is selective for human CD40 and does not involve the IgG (Fc) domain of recombinant human CD40-IgG.

Competition studies revealed an inhibitory concentration (IC50) for NP31 of 215nmol/L, which is comparable to the potency of NP31-strepPE binding to L-CD40 cells and to the IC50 value obtained in the phage displacement studies. Tetrameric NP31-streptavidin complex, prepared by pre-incubation of NP31-biotin for 2h at RT with streptavidin at a 4:1 molar ratio, displayed a minor, 2.5 fold

higher affinity than monomeric NP31 (figure 3.2D, IC50=84nmol/L), pointing to a stochastic rather than multimeric effect.

To pinpoint crucial amino acids and establish the minimal binding motif within NP31 we next performed truncation and alanine scan studies by displacement of NP31-strepHRP binding (250nmol/L) to CD40 with 1µmol/L NP31 or the NP31 analogues (figure 3.2B-C). Alanine substitution confirmed the absolute requirement of a cyclic peptide configuration for effective CD40 binding. The C-terminal amino acids of NP31 seemed to be essential as well as alanine replacements in this part were not tolerated. An N-terminal Glu (4) was found to be preferred. Stepwise truncation of the N-terminal end of NP31 showed that up to 4 amino acid truncations did not markedly affect the affinity for CD40, indicating that presentation of the C-terminal part of NP31 is crucial for CD40 binding. Gly (5) and Ser (6) were replaceable by Ala but could not be left out. Collectively, the truncation and alanine scan studies identify C(x1x2)WRKWVMWGGC as the essential motif for selective CD40 binding, where x can be any amino acid and might in fact only function to provide a proper spatial configuration of the cyclic peptide. This motif correlates very well with the shared peptide motif encoded by the CD40 binding phage clones (Table 3.1).

Table 1 Alignment of CD40 binding peptide sequence selected by phage display

Library	Phage clone	Name
PIF15	DGNVVTCWACREKRW	NP2
pComb8	CMSYEGSWRKWVMWGGC	NP31
	CDLFVMAVGTNLDWWGC	NP26
	CVERCLASTSSGVKALC	NP58
ABC transporter	MSY----RYHWVMWG	

NP31 inhibits CD40L induced VEGF activation and IL-6 production in endothelial cells

Ligation of CD40 in endothelial cells was shown to induce the expression of vascular endothelial growth factor (VEGF) at a transcriptional level[32]. Hence human endothelial cells Ea.Hy.926 were transfected with a VEGF reporter construct at which luciferase expression is under control of the VEGF promoter and the capacity of NP31 to interfere with CD40 activation was assessed. Luciferase activity was seen to be induced in hsCD40L treated versus nontreated or NP31 alone treated EC. NP31 at a concentration of 10µmol/L completely abrogated transcriptional activation of VEGF (figure 3.3A). Similar findings were obtained in CD40L activated murine H5V endothelial cells, suggestive of antagonistic activity of NP31 on mouse CD40. Interestingly, C-terminal biotinylated NP31 monomer prevented VEGF activation at concentrations as low as 100nM (figure

3.3B). In keeping with the displacement studies, the inhibitory effect of NP31 was potentiated by tetrameric presentation on a streptavidin scaffold (figure 3.3C). The enhanced potency did not result from streptavidin itself as the latter did not noticeably affect VEGF activation at 1μM.

In a subsequent study we looked into CD40 dependent production of the proinflammatory cytokine IL-6 by endothelial cells. In line with previous studies, recombinant soluble CD40L strongly induced IL-6 release by human and murine endothelial cells[12]. This induction was dose-dependently inhibited by NP31 (P=0.001, figure 3.3D-E) while 1mM NP31 alone showed no effect on IL-6 production. However, NP31 only conferred partial, 25% reduction of sCD40L induced IL-6 production.

We finally assessed if NP31 acts as a direct antagonist of CD40L/CD40 interaction. Both CD40L antibody LL48 and recombinant CD40-IgG protein showed high binding to L-CD40L cells overexpressing human CD40L. Surprisingly, NP31 up to 10μM was unable to block binding of CD40-IgG to L-CD40L cells (figure 3.3F) suggesting that NP31 does not directly interfere with CD40-CD40L interaction. Conceivably, NP31 acts as an antagonist of CD40 signalling in endothelial cells but with only partial effect. In further studies we concentrated on the potential of NP31 in CD40 directed drug delivery or molecular imaging agent.

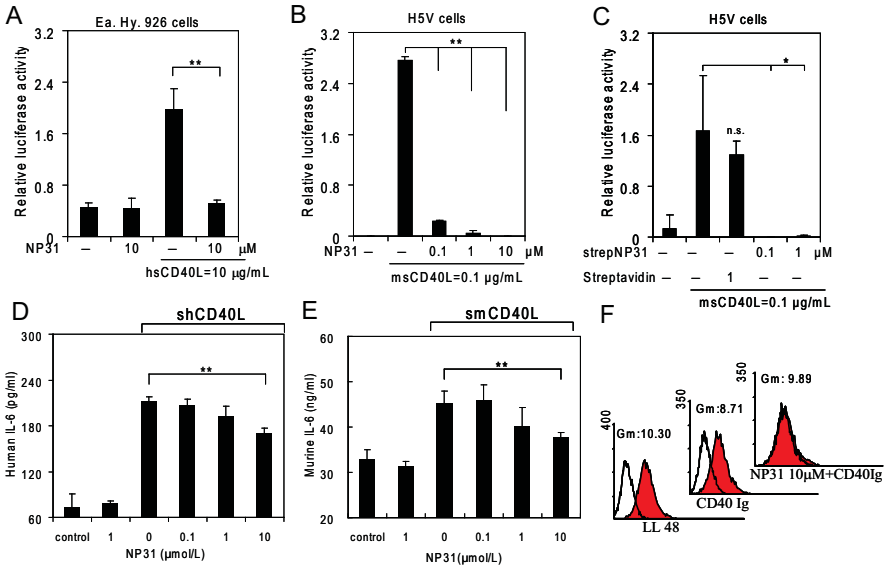

Figure 3.3 NP31 blocks VEGF transcriptional activation and partially inhibits soluble CD40L elicited IL6 production in endothelial cells. Dual luciferase VEGF reporter gene assay was used as readout to measure the functional activity of NP31 on CD40 signalling in human endothelial Ea.hy.926 cells (**A**) and murine endothelial H5V cells **(B, C)** after CD40 ligation. Cells were transiently transfected with pVEGF-luc and pRL-CMV and then stimulated with soluble CD40L at indicated concentrations. Peptides were added at the indicated concentrations together with the soluble recombinant CD40L. Cells lysates were assayed for dual luciferase activity after 12 h. Firefly luciferase activity was normalized for the Renilla luciferase activity. Values are expressed as luciferase units relative to that of stimulated cells and represent means±SD of three independent experiments. **(D)** Ea.Hy.926 and **(E)** H5V cells, cultured in 24 well plates, were treated with shCD40L or smCD40L (10 ng/mL), respectively, in the presence of NP31 at the indicated concentrations. After 24 h, media were collected and IL-6 that had been released into the culture medium was measured by ELISA. Values represent means ±SD of three individual experiments.

CD40 binding phage targets inflamed arthritic joints in a K/BxN mouse model of rheumatoid arthritis

First, we examined the capacity of the CD40 binding phage clone to accumulate in inflamed knee joints in a mouse model of rheumatoid arthritis (figure 3.4A). The K/BxN mouse model has previously been demonstrated to represent an aggressive form of rheumatoid arthritis and the underlying inflammatory response was shown to be CD40 mediated[33, 34]. Tissue analysis two hours after iv injection revealed that radiolabeled NP31 phage displayed a significant, 10-fold increased accumulation in inflamed (summed front and hind limb joints) compared to normal knee joints ((P=0.024; figure 3.4B). Accumulation of control phage by joint was slightly increased as well, which is likely due to enhanced vascular permeability and/or the abundant presence of phagocytotic macrophages in the inflamed tissue, albeit that this effect did not reach significance. Importantly, accumulation of NP31 and control phage in non-inflamed joints did not differ. Moreover, no differences were observed in the tissue distribution profile of NP31 and control phage, and for both phage liver and spleen appeared to be the most prominent sites of phage uptake (figure 3.4C).

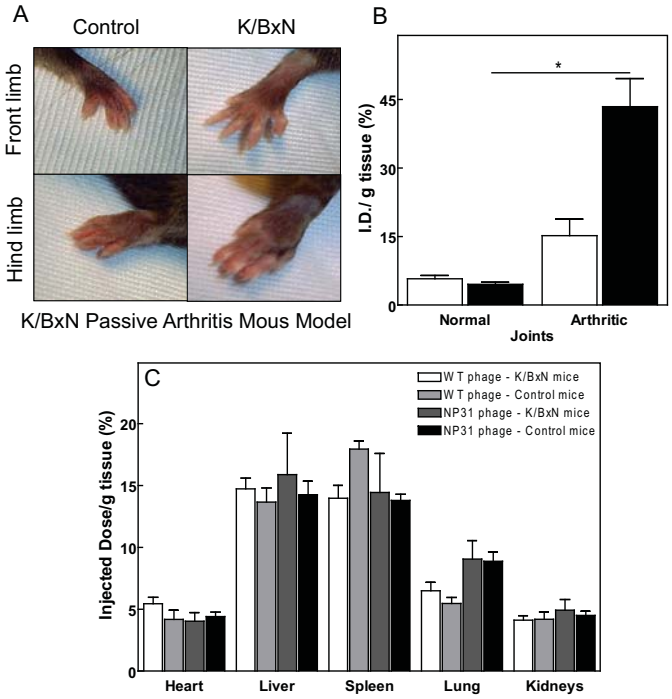

Figure 3.4 CD40 specific NP31 phage home to arthritic joints in a K/BxN mouse model of rheumatoid arthritis. (A) Representative pictures of joints of healthy C57Bl/6 mice which develop acute joints inflammation after intravenous injection of sera from arthritic K/BxN mice. ^{35}S labelled NP31 phage (~200,000 DPM, black bars) and non-specific control phage (eluted from the second round of selection; ~200,000 DPM, open bars) were intravenously injected into C57Bl/6 and K/BxN mice (on a C57Bl/6 background, n=3). After 2 h of circulation, mice were subsequently perfused with DMEM and PBS, organs were removed and the distribution pattern of organ associated radioactivity in mouse joints **(B)** and main organs **(C)** was determined as a percentage of the injected dose/g tissue. Values represent means ±SD.

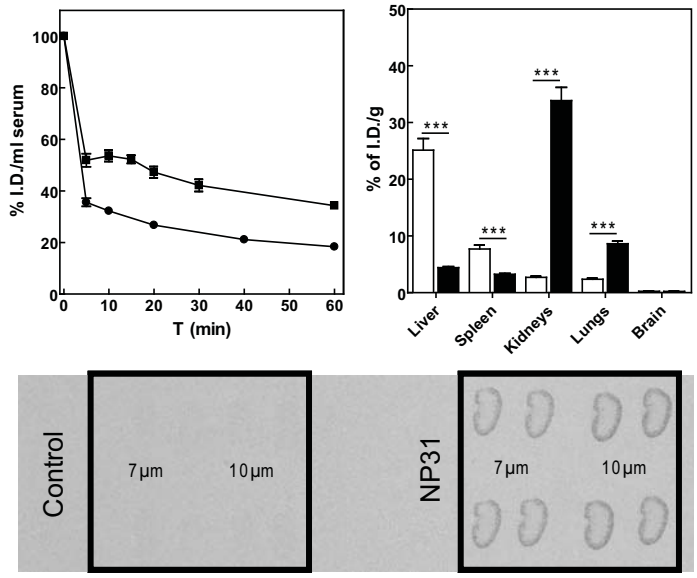

Figure 3.5 In vivo kinetics of NP31 was characterized by serum decay (A) and tissue distribution (B) after intravenously injecting ^{125}I strepNP31 or ^{125}I strepbiotin into ApoE$^{-/-}$ mice. The marked accumulation of strepNP31 in the kidneys was found to mostly reside in the cortex area (C).

Pharmacokinetics and tissue distribution of NP31 peptide in vivo

As a next step we characterized the *in vivo* kinetics of NP31 peptide rather than phage clone. ^{125}I streptavidin conjugated NP31 or biotin was intravenously injected into ApoE$^{-/-}$ mice and serum recovery of targeted and non-targeted streptavidin was determined at the indicated time points (figure 3.5A). NP31 facilitated the initial phase fast distribution of streptavidin with a half life shorter than 3 min. In contrast, streptavidin exhibited a passive *in vivo* uptake pattern with a much longer half life (~20 min) and slower distribution. The recovery of NP31 targeted streptavidin was consistently faster than nontargeted group throughout the time span. The bulky streptavidin nevertheless slows down the clearance of NP31 as seen by 20% residue presence of strepNP31 after 1h circulation. The rapid clearance of NP31 targeted versus nontargeted streptavidin was accompanied by a changed biodistribution profile. Upon intravenously (i.v.) injection, the streptavidin-biotin control was mainly cleared by liver and spleen. NP31 markedly changed the *in vivo* kinetics of streptavidin, with an approximately 10- and 3-fold higher accumulation in kidneys and lungs ($P<0.001$). Uptake and clearance of ^{125}I-strepNP31 by liver and spleen was sharply reduced in comparison with the biotin control (figure 3.5B). To exclude the possibility that the high kidney accumulation of NP31 targeted-streptavidin was a result of blood infiltration, we examined kidney tissue histologically and by autoradiography. In comparison with streptavidin, autoradiography of kidney of NP31 targeted streptavidin showed a significantly higher amount of radioactivity in the renal cortex (figure 3.5C), which is compatible with the previously described abundant CD40 expression in kidney epithelial cells[35].

CD40 targeted imaging of atherosclerotic plaques by NP31

CD40 was shown to be highly expressed on atheroma-associated EC, SMCs and macrophages and in fact it is abundantly present in atheromas of hypercholesterolemic mice, colocalizing with areas of prominent inflammation[12, 17]. To assess the capacity of NP31 for CD40 directed molecular imaging of highly inflammatory atherosclerotic lesions, we intravenously injected streptavidin-PE labelled NP31 (strepPE-NP31) into ApoE$^{-/-}$ mice. Nontargeted strepPE served as a control. Fluorescent image analysis of aorta sections of ApoE$^{-/-}$ mice showed clear peptide accumulation in the atherosclerotic lesion area (figure 3.6B) as a pink overlay of PE (red) and DAPI nuclei staining (blue). After docking of NP31 strepPE signal largely resided in subendothelial tissue. In contrast, nontargeted strepPE was barely detectable in plaques (figure 3.6A). Quantitative analysis showed no difference in plaque size between strepPE control and strepPE-NP31 treated mice. However, NP31 resulted in an approximate 3-fold increase of PE signal in the plaque as expressed as a percentage of the total plaque area. (figure 3.6C-D). Furthermore, immunostaining demonstrated overt colocalization (yellow overlay) of CD40 positive cells (green for CD40 and blue for nucleic DAPI staining) and strepPE-NP31 (red) (figure 3.6E-G). Importantly, NP31 directed PE signal only colocalized with CD40 positive but not with CD40 negative intimal cells. Taken together, these data strongly suggest that NP31 induced homing to atherosclerotic lesions is CD40 mediated.

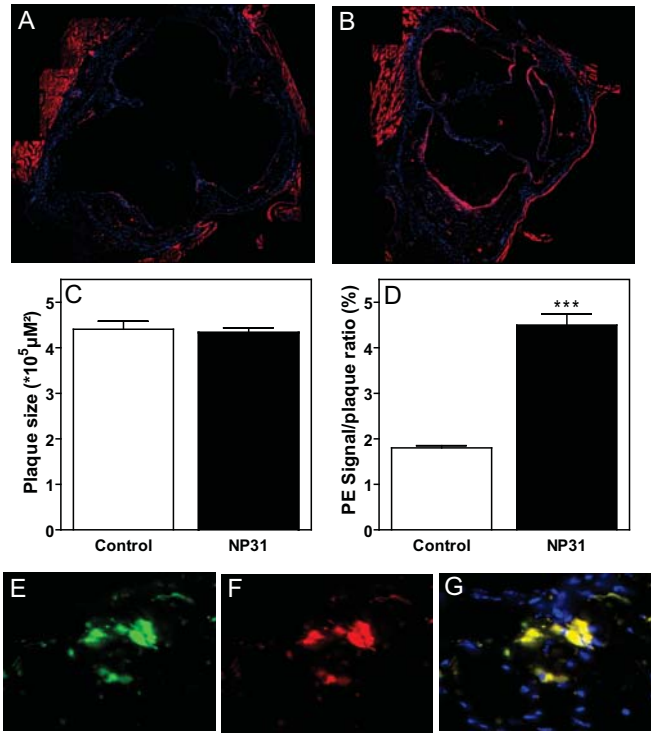

Figure 3.6 Streptavidin-PE docked NP31 colocalizes with atheroma cells in a CD40 dependent manner. (A) Streptavidin PE conjugated NP31-biotin (n=8) or **(B)** biotin alone as a control (n=4) was administered by tail vein injection to ApoE$^{-/-}$ mice. Mice were sacrificed and organs were harvested 1 h after injection. Representative immunofluorescent photomicrographs of aortic sections after strepPE-biotin or strepPE-NP31 injection were shown in upper left and lower left panel, respectively (Magnification: 10x). The strepPE positive area was shown by white arrows. Quantitative analysis of the plaque size and PE signal as a percentage of the total plaque size were given in **C** and **D.** Values represent means±SEM (n=8). Representative merged photomicrographs of cryosections stained for cells expressing CD40 (green), NP31 uptake by PE fluorescence (red) and nuclei by DAPI (blue) were given in **E, F, G,** respectively. Colocalization of atheroma cells with NP31 was shown as an overlay (yellow) (Magnification: 20x).

NP31 peptide targets atherosclerotic aortic artery lesions in ApoE$^{-/-}$ mice

As CD40 was reported to be overexpressed in atherosclerotic lesions and in particular at sites of prominent inflammation[4, 5], we examined the capacity of NP31 to target aortic artery lesions in ApoE$^{-/-}$ mice. Lesion burden, expressed as relative Oil Red O stained aortic area, amounted approximately 15% (figure 3.7). Importantly, although plaque size in both treated groups did not differ, accumulation of radioactivity in aortas after ^{125}I strep-NP31 (n=5) injection was more than two-fold higher than that after injection of ^{125}I strep-biotin (n=5, P<0.001). The arterial distribution pattern of targeted streptavidin was in accordance with that of lipid deposition. We conclude that NP31 facilitates the targeting of carriers to atherosclerotic lesions by direct targeting to CD40.

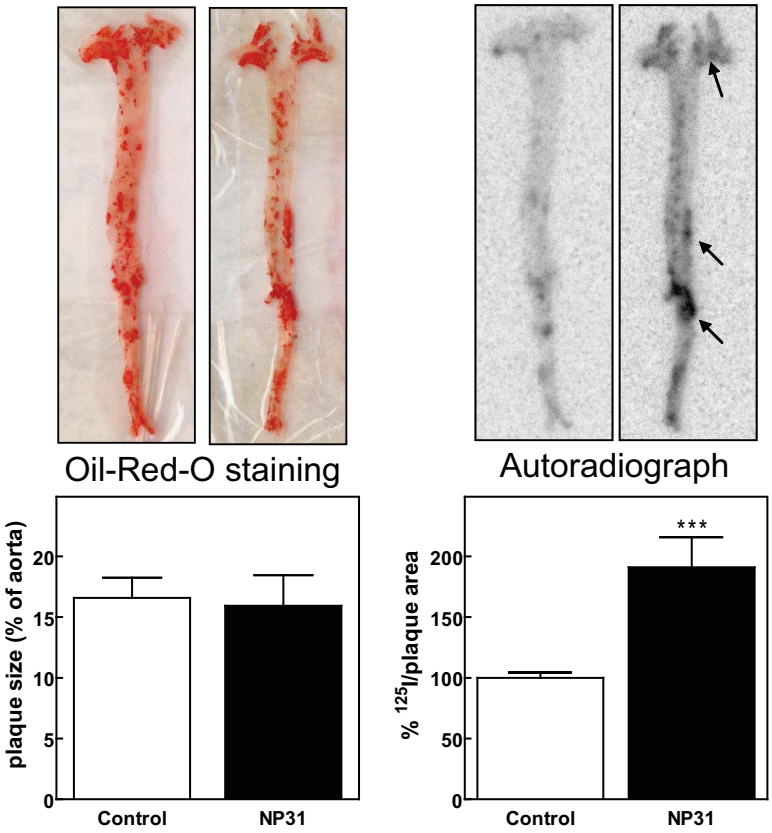

Figure 3.7 NP31 selectively targets atherosclerotic aortic lesions in ApoE$^{-/-}$ mice. ^{125}I strep-biotin or ^{125}I strepNP31 (17 nmol/L) was intravenously injected into aged ApoE$^{-/-}$ mice (~41 weeks old, chow diet, n=5). Representative photomicrographs of tissue sections of longitudinally cut aortas stained for lipid composition with Oil Red O and radiolabeled NP31 distribution stained with autoradiogram were shown in upper and lower left, respectively. Relative lesion area (Lipid staining by ORO as a percentage of total aortic area; open bars) and the autoradiogram signal (as a percentage of the maximal signal in ^{125}I strepNP31 treated group; black bars) are given in the right panel (Values represent means ±SEM ***: P<0.001). Atherosclerotic lesion area with high signal of NP31 was indicated by black arrows.

Discussion

CD40 signalling plays a key role in various inflammatory diseases such as atherosclerosis and rheumatoid arthritis[5, 36]. Studies in mice in which the CD40/CD40L dyad was genetically or functionally disrupted have firmly established the beneficial effect of blockade CD40 ligation for autoimmune diseases and atherosclerosis, in particular plaque stability[19, 20]. Therefore, intervention strategies focusing at the inhibition of CD40 activation hold promise for the treatment of autoimmune diseases. Indeed CD40 directed antibody therapy proved effective in several immune related ailments but unfortunately suffered from severe side effects such as thromboembolism[23]. Moreover the fact that CD40 is overexpressed in all major inflammatory cell types (e.g. macrophages, B-cells, T-cells) and causally implicated in many inflammatory processes, renders it an attractive target for molecular imaging of acute inflammatory processes such as apparent in highly inflammatory vulnerable plaques as well. Thus a need exists for selective CD40 antagonists which do not compromise platelet activity but bind CD40 to inhibit CD40 mediated inflammatory responses. In this paper, we describe the identification of a 15-mer constrained peptide, which selectively binds to human CD40 with nanomolar affinity to confer full inhibition of CD40L induced VEGF activation and partial inhibition of CD40L induced IL-6 responses. This peptide ligand conveys phage as well as other carriers such as streptavidin specifically to sites of inflammation such as the knee joints in a mouse model of rheumatoid arthritis and atherosclerotic plaques in ApoE$^{-/-}$ mice.

Unbiased combinatorial phage display technology was employed to identify novel peptide ligands with high specificity and potency for CD40, The consensus motif WRKWVMWG is relatively rich in tryptophans and basic amino acids. A synthetic peptide encompassing the WRKWVMWG core motif (NP31) bound selectively and avidly to CD40 at an IC_{50} of 215-440nM as judged from phage and streptavidin-HRP displacement assays. FACS analysis confirmed that NP31 interacted with CD40 expressing cells. NP31, when docked onto a streptavidin template displayed even higher affinity for human CD40, confirming the importance of multimerization for CD40 recognition.

In view of the bulky size and trimeric configuration of CD40L, it is not surprising that ligand design for CD40 has been rather unsuccessful. Until now, small molecule inhibitors for CD40 have not been reported. Efforts had only led to identification of a linear CD40 binding peptide containing FPGN motif[37], which does not show any homology to NP31, pointing a separate binding sites on CD40. Although FPGN peptide was able to enhance the adenoviral infection of dendritic cells in vitro, it was nonselective and of low affinity. As compared to FPGN, NP31 displayed superior specificity and nanomolar potency for CD40.

Previously, homologues modeling studies have revealed that the interface of CD40/CD40L complexes comprises a high density of charged residues, with CD40L and CD40 presenting basic (K143, R203, R207) and acidic side chains

(D84, E114, E117), respectively[38]. In keeping the 11-mer GSWRKWVMWGG core motif identified by truncation and alanine scan indeed confirmed the critical importance of the C-terminal basic amino acids in CD40 recognition. Thus it is tempting to assume that the basic amino acids within NP31 interact with a complementary stretch of acidic amino acids within the binding pocket of CD40. This notion is seemingly contradicted by our finding that NP31 is unable to disrupt CD40L binding, although NP31 peptide might not necessarily occupy the complete CD40L binding pocket to interdict part of the conformational changes and thus signal transduction pathways induced by CD40L. Alternatively NP31 may be too small to prevent the proposed multi-site access of CD40L to CD40[30] or interact at a unique binding pocket on CD40 that is not directly involved in CD40L binding.

CD40 signalling is a complex and only partially understood process and is context as well as cell type dependent[39, 40]. The observed discrepancy between complete antagonism of VEGF transcription and partial of CD40 dependent IL-6 activation by NP31 might arise from differential interference with TRAF signaling partners in EC. For example, VEGF transcription is not mediated by nuclear factor (NF)-κB[32] and may thus proceed through TRAF2. In contrast, IL-6 activation after CD40 engagement was found to be involve TRAF6 dependent NF-κB activation[41]. NP31 seemed to be unable to inhibiting IgA production by B cells or dendritic cells after CD40L activation (data not shown). Altogether, our data suggest that NP31 acts as a selective, but partial CD40 antagonist in endothelial cells.

High risk plaques are often moderately stenotic and highly inflammatory in nature. They are barely detectable by conventional angiographic measures. Given their high inflammatory cell content, molecular imaging efforts that target on inflammatory markers may be particularly discriminative. For example passive targeting of plaque macrophages as well as adhesion molecules, macrophage scavenger receptors, integrins, oxidation, apoptosis and protease[42-46] have been studied in this regard. As CD40 has been functionally implicated in plaque destabilisation, it is tempting to assume that it constitutes a better candidate to define the vulnerable plaque. A second advantage of CD40 targeted imaging will be a direct delineation of atherosclerotic inflammation instead of evaluation lipid deposition or macrophage infiltration. Finally, although specific and potent monoclonal CD40 antibodies are available for targeted imaging, they are suffering from large size, potential immunogenicity, slow kinetics and thus high signal-to-noise ratio *in vivo*. A small peptide, NP31 may contrast favourably to CD40 antibodies in terms of accessible and controlled synthesis, flexibility, size and pharmacokinetics.

In conclusion, we here describe the design by phage display of a novel peptide NP31 which displays nanomolar affinity for human CD40 and antagonizes part of the CD40L induced cytokine responses. From truncation and alanine studies we identify an 11-mer core motif within NP31 to suffice for high affinity binding. Furthermore, we show that NP31 can redirect phage as well as streptavidin scaffolds to sites of inflammation such as atherosclerotic plaques in a CD40 dependent manner. We propose that NP31 or NP31 peptidomimetics may by virtue of their synthetic accessibility, homing capacity and partial antagonistic activity allow targeted diagnosis of and intervention in inflammatory disorders such as atherosclerosis and autoimmune disease.

Sources of Funding

This study was financially supported by grants LFA5952 from Technology Foundation STW. This study was also supported by generous grants 2003T.201 (EB) from the Netherlands Heart Foundation. The authors belong to the European Vascular Genomics Network (http://www.evgn.org), a Network of Excellence supported by the European Community's Sixth Framework Program for Research Priority 1 (Life Sciences, Genomics, and Biotechnology for Health; contract LSHM-CT-2003-503254).

References

1. Van Kooten C, Banchereau J. CD40-CD40 ligand: a multifunctional receptor-ligand pair. *Adv Immunol.* 1996;61:1-77.
2. Clark LB, Foy TM, Noelle RJ. CD40 and its ligand. *Adv Immunol.* 1996;63:43-78.
3. Grewal IS, Flavell RA. CD40 and CD154 in cell-mediated immunity. *Annu Rev Immunol.* 1998;16:111-135.
4. Schonbeck U, Libby P. The CD40/CD154 receptor/ligand dyad. *Cell Mol Life Sci.* 2001;58:4-43.
5. Schonbeck U, Libby P. CD40 signaling and plaque instability. *Circ Res.* 2001;89:1092-1103.
6. Alderson MR, Armitage RJ, Tough TW, Strockbine L, Fanslow WC, Spriggs MK. CD40 expression by human monocytes: regulation by cytokines and activation of monocytes by the ligand for CD40. *J Exp Med.* 1993;178:669-674.
7. Bruemmer D, Riggers U, Holzmeister J, Grill M, Lippek F, Settmacher U, Regitz-Zagrosek V, Fleck E, Graf K. Expression of CD40 in vascular smooth muscle cells and macrophages is associated with early development of human atherosclerotic lesions. *Am J Cardiol.* 2001;87:21-27.
8. Hollenbaugh D, Mischel-Petty N, Edwards CP, Simon JC, Denfeld RW, Kiener PA, Aruffo A. Expression of functional CD40 by vascular endothelial cells. *J Exp Med.* 1995;182:33-40.
9. Karmann K, Hughes CC, Schechner J, Fanslow WC, Pober JS. CD40 on human endothelial cells: inducibility by cytokines and functional regulation of adhesion molecule expression. *Proc Natl Acad Sci U S A.* 1995;92:4342-4346.
10. Krzesz R, Wagner AH, Cattaruzza M, Hecker M. Cytokine-inducible CD40 gene expression in vascular smooth muscle cells is mediated by nuclear factor kappaB and signal transducer and activation of transcription-1. *FEBS Lett.* 1999;453:191-196.
11. Yellin MJ, Brett J, Baum D, Matsushima A, Szabolcs M, Stern D, Chess L. Functional interactions of T cells with endothelial cells: the role of CD40L-CD40-mediated signals. *J Exp Med.* 1995;182:1857-1864.
12. Mach F, Schonbeck U, Sukhova GK, Bourcier T, Bonnefoy JY, Pober JS, Libby P. Functional CD40 ligand is expressed on human vascular endothelial cells, smooth muscle cells, and macrophages: implications for CD40-CD40 ligand signaling in atherosclerosis. *Proc Natl Acad Sci U S A.* 1997;94:1931-1936.
13. Aruffo A, Farrington M, Hollenbaugh D, Li X, Milatovich A, Nonoyama S, Bajorath J, Grosmaire LS, Stenkamp R, Neubauer M, et al. The CD40 ligand, gp39, is defective in activated T cells from patients with X-linked hyper-IgM syndrome. *Cell.* 1993;72:291-300.
14. Gerritse K, Laman JD, Noelle RJ, Aruffo A, Ledbetter JA, Boersma WJ, Claassen E. CD40-CD40 ligand interactions in experimental allergic encephalomyelitis and multiple sclerosis. *Proc Natl Acad Sci U S A.* 1996;93:2499-2504.
15. Larsen CP, Elwood ET, Alexander DZ, Ritchie SC, Hendrix R, Tucker-Burden C, Cho HR, Aruffo A, Hollenbaugh D, Linsley PS, Winn KJ, Pearson TC. Long-term acceptance of skin and cardiac allografts after blocking CD40 and CD28 pathways. *Nature.* 1996;381:434-438.
16. Lutgens E, Gorelik L, Daemen MJ, de Muinck ED, Grewal IS, Koteliansky VE, Flavell RA. Requirement for CD154 in the progression of atherosclerosis. *Nat Med.* 1999;5:1313-1316.
17. Mach F, Schonbeck U, Sukhova GK, Atkinson E, Libby P. Reduction of atherosclerosis in mice by inhibition of CD40 signalling. *Nature.* 1998;394:200-203.
18. Durie FH, Fava RA, Foy TM, Aruffo A, Ledbetter JA, Noelle RJ. Prevention of collagen-induced arthritis with an antibody to gp39, the ligand for CD40. *Science.* 1993;261:1328-1330.
19. Kirk AD, Burkly LC, Batty DS, Baumgartner RE, Berning JD, Buchanan K, Fechner JH, Jr., Germond RL, Kampen RL, Patterson NB, Swanson SJ, Tadaki DK, TenHoor CN, White L, Knechtle SJ, Harlan DM. Treatment with humanized monoclonal antibody against CD154 prevents acute renal allograft rejection in nonhuman primates. *Nat Med.* 1999;5:686-693.
20. Kenyon NS, Fernandez LA, Lehmann R, Masetti M, Ranuncoli A, Chatzipetrou M, Iaria G, Han D, Wagner JL, Ruiz P, Berho M, Inverardi L, Alejandro R, Mintz DH, Kirk AD, Harlan DM, Burkly LC, Ricordi C. Long-term survival and function of intrahepatic islet allografts in baboons treated with humanized anti-CD154. *Diabetes.* 1999;48:1473-1481.
21. Schonbeck U, Sukhova GK, Shimizu K, Mach F, Libby P. Inhibition of CD40 signaling limits evolution of established atherosclerosis in mice. *Proc Natl Acad Sci U S A.* 2000;97:7458-7463.

22. Lutgens E, Cleutjens KB, Heeneman S, Koteliansky VE, Burkly LC, Daemen MJ. Both early and delayed anti-CD40L antibody treatment induces a stable plaque phenotype. *Proc Natl Acad Sci U S A.* 2000;97:7464-7469.

23. Kawai T, Andrews D, Colvin RB, Sachs DH, Cosimi AB. Thromboembolic complications after treatment with monoclonal antibody against CD40 ligand. *Nat Med.* 2000;6:114.

24. Tai YT, Podar K, Gupta D, Lin B, Young G, Akiyama M, Anderson KC. CD40 activation induces p53-dependent vascular endothelial growth factor secretion in human multiple myeloma cells. *Blood.* 2002;99:1419-1427.

25. van Kooten C, Gerritsma JS, Paape ME, van Es LA, Banchereau J, Daha MR. Possible role for CD40-CD40L in the regulation of interstitial infiltration in the kidney. *Kidney Int.* 1997;51:711-721.

26. Molenaar TJ, Appeldoorn CC, de Haas SA, Michon IN, Bonnefoy A, Hoylaerts MF, Pannekoek H, van Berkel TJ, Kuiper J, Biessen EA. Specific inhibition of P-selectin-mediated cell adhesion by phage display-derived peptide antagonists. *Blood.* 2002;100:3570-3577.

27. Yu H, Sliedregt-Bol K, Overkleeft H, van der Marel GA, van Berkel TJ, Biessen EA. Therapeutic potential of a synthetic peptide inhibitor of nuclear factor of activated T cells as antirestenotic agent. *Arterioscler Thromb Vasc Biol.* 2006;26:1531-1537.

28. Boross P, Verbeek JS. The complex role of Fcgamma receptors in the pathology of arthritis. *Springer Semin Immunopathol.* 2006;28:339-350.

29. Molenaar TJ, Michon I, de Haas SA, van Berkel TJ, Kuiper J, Biessen EA. Uptake and processing of modified bacteriophage M13 in mice: implications for phage display. *Virology.* 2002;293:182-191.

30. Chan FK, Chun HJ, Zheng L, Siegel RM, Bui KL, Lenardo MJ. A domain in TNF receptors that mediates ligand-independent receptor assembly and signaling. *Science.* 2000;288:2351-2354.

31. Pearson AM, Rich A, Krieger M. Polynucleotide binding to macrophage scavenger receptors depends on the formation of base-quartet-stabilized four-stranded helices. *J Biol Chem.* 1993;268:3546-3554.

32. Melter M, Reinders ME, Sho M, Pal S, Geehan C, Denton MD, Mukhopadhyay D, Briscoe DM. Ligation of CD40 induces the expression of vascular endothelial growth factor by endothelial cells and monocytes and promotes angiogenesis in vivo. *Blood.* 2000;96:3801-3808.

33. Kyburz D, Carson DA, Corr M. The role of CD40 ligand and tumor necrosis factor alpha signaling in the transgenic K/BxN mouse model of rheumatoid arthritis. *Arthritis Rheum.* 2000;43:2571-2577.

34. Ditzel HJ. The K/BxN mouse: a model of human inflammatory arthritis. *Trends Mol Med.* 2004;10:40-45.

35. van Kooten C, Woltman AM, Daha MR. Immunological function of tubular epithelial cells: the functional implications of CD40 expression. *Exp Nephrol.* 2000;8:203-207.

36. Korganow AS, Ji H, Mangialaio S, Duchatelle V, Pelanda R, Martin T, Degott C, Kikutani H, Rajewsky K, Pasquali JL, Benoist C, Mathis D. From systemic T cell self-reactivity to organ-specific autoimmune disease via immunoglobulins. *Immunity.* 1999;10:451-461.

37. Richards JL, Abend JR, Miller ML, Chakraborty-Sett S, Dewhurst S, Whetter LE. A peptide containing a novel FPGN CD40-binding sequence enhances adenoviral infection of murine and human dendritic cells. *Eur J Biochem.* 2003;270:2287-2294.

38. Singh J, Garber E, Van Vlijmen H, Karpusas M, Hsu YM, Zheng Z, Naismith JH, Thomas D. The role of polar interactions in the molecular recognition of CD40L with its receptor CD40. *Protein Sci.* 1998;7:1124-1135.

39. Harnett MM. CD40: a growing cytoplasmic tale. *Sci STKE.* 2004;2004:pe25.

40. Zirlik A, Bavendiek U, Libby P, MacFarlane L, Gerdes N, Jagielska J, Ernst S, Aikawa M, Nakano H, Tsitsikov E, Schonbeck U. TRAF-1, -2, -3, -5, and -6 are induced in atherosclerotic plaques and differentially mediate proinflammatory functions of CD40L in endothelial cells. *Arterioscler Thromb Vasc Biol.* 2007;27:1101-1107.

41. Baccam M, Woo SY, Vinson C, Bishop GA. CD40-mediated transcriptional regulation of the IL-6 gene in B lymphocytes: involvement of NF-kappa B, AP-1, and C/EBP. *J Immunol.* 2003;170:3099-3108.

42. Jaffer FA, Libby P, Weissleder R. Molecular imaging of cardiovascular disease. *Circulation.* 2007;116:1052-1061.

43. Jaffer FA, Libby P, Weissleder R. Molecular and cellular imaging of atherosclerosis: emerging applications. *J Am Coll Cardiol.* 2006;47:1328-1338.

44. Amirbekian V, Lipinski MJ, Briley-Saebo KC, Amirbekian S, Aguinaldo JG, Weinreb DB, Vucic E, Frias JC, Hyafil F, Mani V, Fisher EA, Fayad ZA. Detecting and assessing macrophages in vivo to evaluate atherosclerosis noninvasively using molecular MRI. *Proc Natl Acad Sci U S A.* 2007;104:961-966.

45. Hyafil F, Cornily JC, Feig JE, Gordon R, Vucic E, Amirbekian V, Fisher EA, Fuster V, Feldman LJ, Fayad ZA. Noninvasive detection of macrophages using a nanoparticulate contrast agent for computed tomography. *Nat Med.* 2007;13:636-641.

46. Kaufmann BA, Sanders JM, Davis C, Xie A, Aldred P, Sarembock IJ, Lindner JR. Molecular imaging of inflammation in atherosclerosis with targeted ultrasound detection of vascular cell adhesion molecule-1. *Circulation.* 2007;116:276-284.